Scientific Journal of Silesian University of Technology. Series Transport
Zeszyty Naukowe Politechniki Śląskiej. Seria Transport

Volume 105 **2019**

p-ISSN: 0209-3324

e-ISSN: 2450-1549

DOI: https://doi.org/10.20858/sjsutst.2019.105.9

Journal homepage: http://sjsutst.polsl.pl

Article citation information:
Konowrocki, R. Modelling of dynamic aspects of operation in railway vehicle traction drive system including the electromechanical coupling. *Scientific Journal of Silesian University of Technology. Series Transport*. 2019, **105**, 101-111. ISSN: 0209-3324.
DOI: https://doi.org/10.20858/sjsutst.2019.105.9.

Robert KONOWROCKI[1]

MODELLING OF DYNAMIC ASPECTS OF OPERATION IN RAILWAY VEHICLE TRACTION DRIVE SYSTEM INCLUDING THE ELECTROMECHANICAL COUPLING

Summary. In this paper, the influence of electromechanical interaction in an electric motor on the railway vehicle driving system dynamics was investigated. This is the train driven by DC. In particular, there is considered influence of electromagnetic field between a rotor and stator on excitation of resonant torsional vibrations of the drive system. Conclusions drawn from the computational results can be very useful during the design phase of these devices as well as helpful for their users during regular maintenance.

Keywords: railway drive system, electromechanical coupling, numerical analysis, electric motor, torsion vibration, railway vehicle operation

1. INTRODUCTION

Torsional vibrations occur in every drive train. For a simple drive train, which consists of an electrical motor, flexible shaft and a load, its system has two basic torsional vibration modes, the rigid-body mode and the first elastic mode. The knowledge about the torsional vibrations in drive transmission systems of railway vehicles is of great importance in the field of dynamics of mechanical systems [3,4,7,8,10,14,15,19]. Components of driving systems are

[1]Institute of Fundamental Technological Research, Polish Academy of Sciences, Pawinskiego 5B Street, 02-106 Warszawa, Poland. Email: rkonow@ippt.pan.pl

not fully rigid, it is common to have fluctuation of torques in different work phases leading to shaft and wheelset torsional vibration [5,11]. For the reliability and security of the drive system of railway vehicles driven by electric motors, the electromagnetic output traction force and torques should drive stably. Otherwise the shaft train vibration caused by motor torque ripple will affect the fatigue life of the drive components and the operation security of the driven railway vehicles [2,9,18]. Generally, railway drive systems can be divided into electrical and mechanical parts, for this reason, the influence of the electric motor should also be taken into account in the dynamic analysis of the drive.

In practice, various types of motors for traction applications are used. Among which are: DC shunt motor, compound motors, separately excited motors, AC series motor, 3-phase induction motor. The selection of motors depends on a variety of factors like the type of traction, type of supply, mainline/suburban trains, etc. The motor should provide high starting torque, which is very essential because in trains there are many compartments full of passengers or goods, so it requires high torque during initial start-up and traction operation. In our case, we will deal with the railway traction system driven by a DC motor. In this paper, the effect of electromechanical coupling in the electric motor on torsion vibration of the railway drive system was analysed. For this analysis, the method presented therein [2] was applied. In the considered model, the magnetic field interaction between the stator and the rotor of the DC motor was considered. Using the energy balance of the natural modes of oscillations for the model of the railway traction drive are obtained expressions for determining the influence of electromagnetic parameters of the electric motor (stiffness and damping of electromagnetic field) on its stability in relation to the torsion vibration of the railway drivelines.

2. THE DRIVETRAIN UNDER INVESTIGATION

For analysis of torsional vibrations in a dynamic mutual coupling between the wheelset and the electric motor, a possibly realistic and reliable electromechanical model of the railway drivetrain was applied. In the study, electric locomotives with the fully sprung wheelset drive were used. In this drive system, the DC traction motor is a drive unit. The motor shaft is connected to the pinion wheel of the gearbox by an elastic coupling. The gearbox provides the transmission of the torque to the wheel axle thus reducing the angular speed. The gear wheel is mounted on a hollow shaft which is coupled to the wheel axle by an elastic coupling. Motor and gearbox housing are connected rigidly to each other and are suspended in the bogie frame by rubber silent blocs (Fig. 1).

3. MATHEMATICAL MODEL OF THE RAILWAY TRACTION DRIVE SYSTEM

The kinematic diagram of the considered railway traction drive system model with a DC motor is depicted in Figure 2. Output shaft of the electric motor is coupled to the hollow shaft connected with the wheelset. The electrical drivetrain shown in Figure 1 can be reduced by assuming infinite gear tooth stiffness and assuming the wheel shaft coupling as a single spring. A simple model of this drive is shown in Figure 2. The output driving torque from the electric motor is transmitted via coupling to the hollow shaft, which surrounds the wheelset axle. On the opposite end of the hollow shaft, the torque is transmitted by means of a flexible claw coupling to the disc-wheel. On the basis of the data on the cross-section area as well as

the length of the hollow shaft and geometry of the wheelset, stiffness of these assembled elements was determined. In the considered model, the toothed gear was omitted, treating it as an element with several times more stiffness than the hollow shaft.

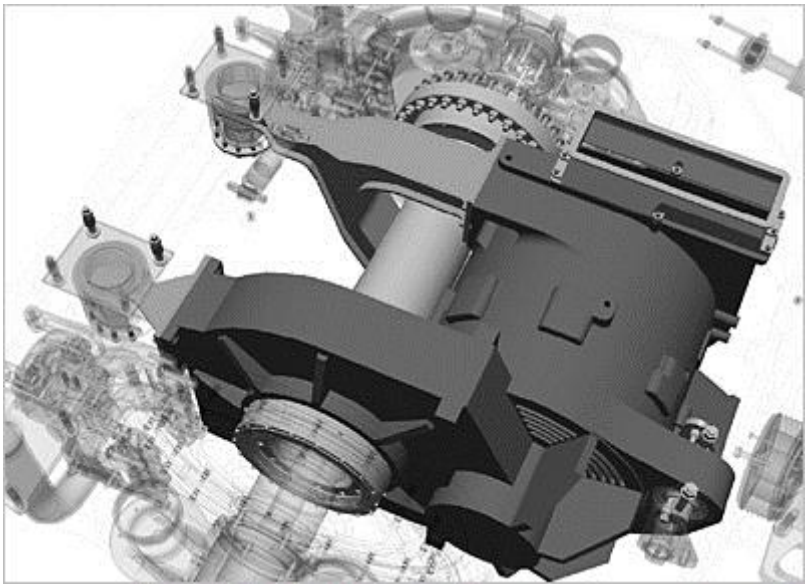

Fig. 1. Railway drive system with hollow shaft transmitted torque [16]

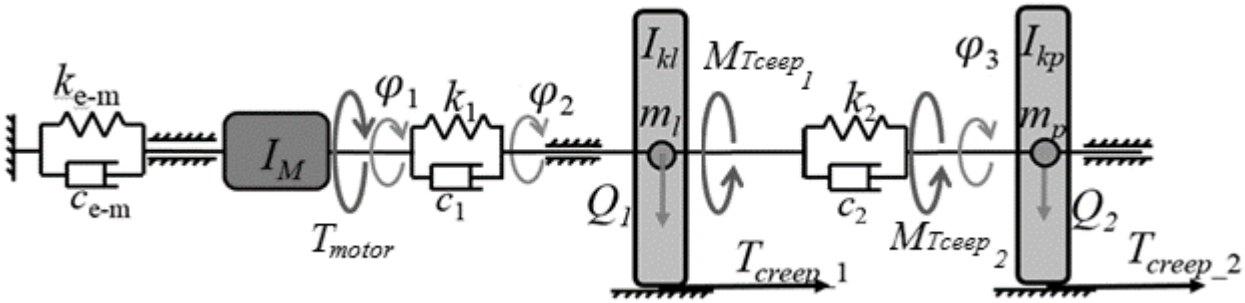

Fig. 2. Scheme of model of railway drive

The equation of motion of the mechanical model shown in Fig 2 can be described in matrix form

$$\mathbf{I}\ddot{\varphi}(\mathrm{t}) = (\mathbf{C}_{e-m} + \mathbf{C}_{coupl} + \mathbf{C}_{wheelset}) \cdot \dot{\varphi}(\mathrm{t}) + (\mathbf{K}_{e-m} + \mathbf{K}_{coupl} + \mathbf{K}_{wheelset}) \cdot \varphi(\mathrm{t}) = \mathbf{T}_{motor} + \mathbf{M}_{Tcreep\_i} \cdot r_i \quad (1)$$

where **I** denotes the mass matrix containing mass moments of inertia of rotating elements of the drive system, the matrixes, $\mathbf{C}_{e\text{-}m}$, $\mathbf{C}_{coupl,}$ $\mathbf{C}_{wheelset}$, $\mathbf{K}_{coupled}$, $\mathbf{K}_{e\text{-}m}$ and $\mathbf{K}_{wheelset}$ represent the torsional damping and stiffness properties of electric motor magnetic field, rotor shaft, the hollow shaft and the wheelset, respectively. Vector $\mathbf{T}_{motor}$ contains the electromagnetic torque generated by the electric motor described in equation (1) of the paper and vector $\mathbf{M}_{creep}$ contains the traction torque generated by longitudinal tangential loads T_{creep_i} in the wheel-rail zones acting on wheel radius r_i.

The electromagnetic torque of DC motor T_{motor}, the stiffness and damping generated by the electromagnetic field between stator and rotor of the motor are defined by equation 2-4, according to Riven [1].

$$T_{motor}(t) = \frac{k_v}{R}\left(U - k_v \cdot \dot{\varphi}_1(t)\right), \tag{2}$$

$$k_{\text{e–m}} = \left[\frac{1}{\omega_0 \cdot p \cdot \tau_e}\right], \tag{3}$$

$$c_{\text{e–m}} = \left[\frac{\tau_e}{I_M}\right], \tag{4}$$

where: $p = T_{motor} / \dot{\varphi}_1$, $\tau_e = L/R$. Parameters k_v, R, L, U, I_M, ω_0, τ_e, p and $\varphi_1(t)$ are respectively constant (ratio of the voltage generated by the motor to the speed), electrical resistance and inductance of the motor windings, the power supply voltage, mass moments of inertia of rotor, no-load speed of the motor, electromagnetic time constants, slope of torque T_{motor} versus slippage characteristic (Fig. 3), angular speed of rotor. $k_{\text{e-m}}(\omega)$ and $c_{\text{e-m}}(\omega)$ are respectively the stiffness and damping coefficients associated with the electromagnetic field. These parameters in the considered model are represented as the viscoelastic electromagnetic clamping of the motor rotor with the immovable stator (Fig. 2). The angular position of the rotor of the DC motor is represented by φ_1 and the angular positions of the wheels of the wheelset are described by φ_2 and φ_3, respectively. I_{kl}, I_{kr} are the mass moment of inertia of the left and right wheel of the wheelset.

Depending on the adopted various maintenance, operation and weather conditions, an adhesion in wheel-rail contact zone characteristic can take into consideration these various forms [17]. The adhesion curve applied for the carried out investigations was plotted in Fig. 3 (left). Presented in the figure are an adhesion and traction characteristic and instantaneous point equilibrium between them. Here, p and η_i meaning respectively, the slope coefficients of the traction characteristics (green curve) and adhesion characteristics (red curve) in the vicinity of the temporary equilibrium point. Example graphs of the driving/electric torque moment T_{motor} and the resistance torque M_{Tcreep} caused by the coefficient of wheel-rail adhesion are shown in Fig 4a and b. These diagrams illustrate the stability of the drive wheel set depending on which of the T_{motor} or M_{Tcreep} torque is larger. Such an appearance has an effect on the torsional vibration of the wheelset.

The matrix form of traction drive model represented by a three-mass rotating system (Fig. 2) can be described by a system of differential equations (5).

$$\begin{cases} \tau_e \cdot \dot{T}_{motor} + T_{motor} = -p \cdot \dot{\varphi}_1 \\ I_M \ddot{\varphi}_1 + k_{e-m} \cdot \varphi_1 + k_1 \cdot (\varphi_1 - \varphi_2) + c_{e-m} \cdot \dot{\varphi}_1 + c_1 \cdot (\dot{\varphi}_1 - \dot{\varphi}_2) = T_{motor} \\ I_{kl} \ddot{\varphi}_2 + k_1 \cdot (\varphi_2 - \varphi_1) + k_2 \cdot (\varphi_2 - \varphi_3) + c_1 \cdot (\dot{\varphi}_2 - \dot{\varphi}_1) + c_2 \cdot (\dot{\varphi}_2 - \dot{\varphi}_3) = \eta_{kl} \cdot \dot{\varphi}_2 \\ I_{kp} \ddot{\varphi}_3 + k_2 \cdot (\varphi_3 - \varphi_2) + c_2 \cdot (\dot{\varphi}_3 - \dot{\varphi}_2) = \eta_{kp} \cdot \dot{\varphi}_3 \end{cases}, \tag{5}$$

where k_2 and c_2 are the stiffness and damping characteristics of the wheelset structure. η_{kp} and η_{kl} coefficients of slope of the adhesion characteristics in the wheel-rail contact area of both wheels. The electromagnetic time constant of the windings τ_e describes the delay of reduce in the current in comparison to the initial value when the voltage is switched at the terminals of DC motor. It is actually the stall current because as soon as the motor starts to rotate, it generates a back electromotive force (EMF) to oppose the applied voltage, which reduces the

actual current flowing. Therefore, for rapid acceleration of a motor, a very high voltage and steady feed of the motor with a constant current circuit is needed.

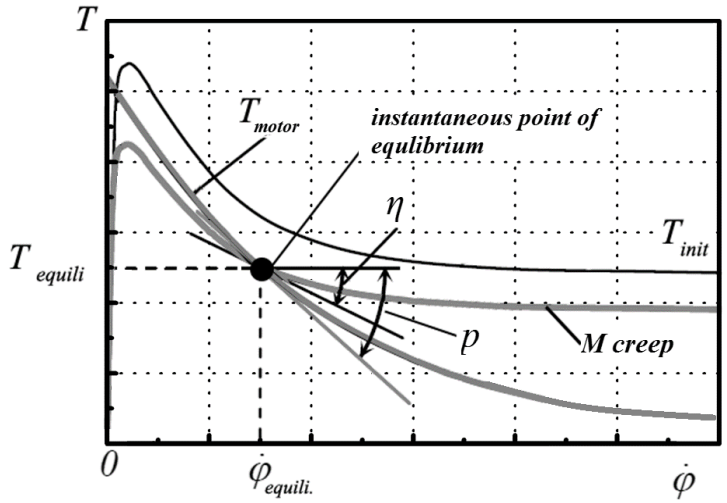

Fig. 3. Equilibrium mode of adhesion and traction characteristic

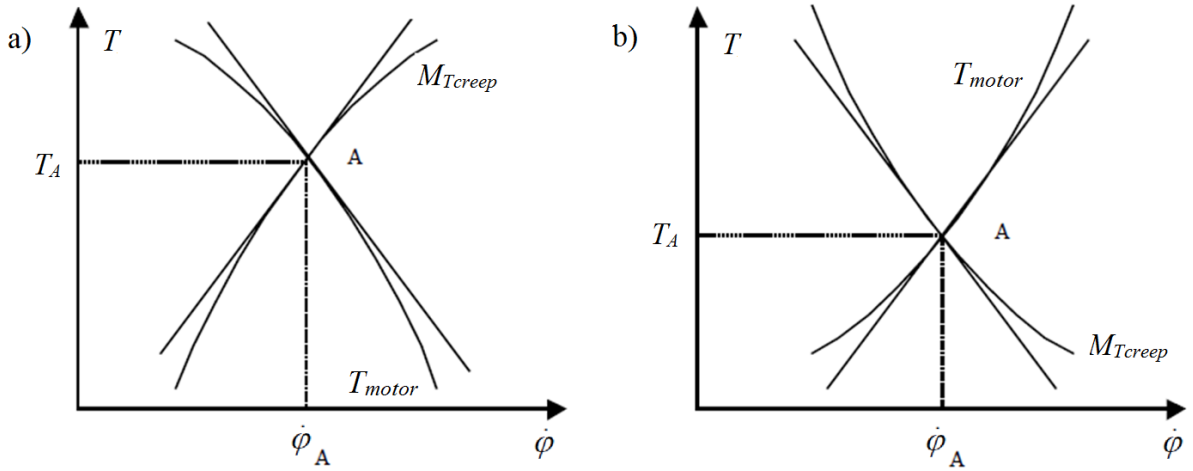

Fig. 4. Example of stability, a) and unstability, b) conditions of the adhesion and traction characteristic [6]

In the considered case, we assume that the conditions of adhesion in wheel-rail zones of both wheels of wheelset are the same. Therefore, we can simplify the considered system by introducing a relationship that $\eta_{kp} = \eta_{kl=} \eta$ (Fig. 3). If the system is on the boundary of stability, the condition of energy balance implies that the average power supplied to the system in the process of self-excited oscillations with i-th natural frequency is equal to the average power dissipated in the process of self-oscillations, a similar approach was used in this paper [12]. Assuming that the generalised coordinates of the model vary harmonically, we define the average for the period of power supplied into the system in the process of self-excited oscillations with natural frequency ω_i

$$E_{self\_i} = \frac{1}{T_i}\int_0^{T_i}[\eta(\phi_2^2(t) - \phi_3^2(t)) \cdot \sin(\omega_i t)]\,dt = 0.5 \cdot \eta(\phi_2^2(t) - \phi_3^2(t)) \,, \tag{6}$$

where T_i describes the period of oscillation with a natural frequency of this system, expressed relation $T_i = 2\pi / \omega_i$. In the considered case, the power dissipated due to mechanical damping of the railway drive elements E_{mech_i} can be determined by equation 7

$$E_{mech} = \frac{1}{T_i}\int_0^{T_i} [c_{e-m} \cdot \phi_1^2(t) + c_1 \cdot (\phi_1(t) - \phi_2(t))^2 + c_2 \cdot (\phi_2(t) - \phi_1(t))^2] \cdot \sin^2(\omega_i t)\, dt$$
$$= \tfrac{1}{2}[c_{e-m} \cdot \phi_1^2(t) + c_1 \cdot (\phi_1(t) - \phi_2(t))^2 + c_2 \cdot (\phi_2(t) - \phi_1(t))^2]. \quad (7)$$

In order to estimate the average over power $E_{e\text{-}mech}$ consumed in the electromechanically interaction in motor, the first equation of system (5) was analysed. In (5), T_{motor} stands for the dissipative torque that reflects the electromechanical coupling in the electric motor. Accordingly, to [12] the average power $E_{e\text{-}mech}$ computed for the oscillation period can be defined as follows:

$$E_{e-mech\_i} = \frac{1}{T_i}\int_0^{T_i} [T_{motor} \cdot \phi_{1i}]\, dt, \quad (8)$$

Introducing the assumption $T_{motor}=T_{motor}\sin(\omega_i t+\psi_i)$, we can estimate the modulus of torque T_{motor}, and solve the first equation of system (5) by employing the method of complex amplitudes, described in detail in this paper [12]. This approach takes into account both the amplitude-frequency characteristic of the inertial link $W(\omega_i)$ and phase angle ψ_i between the velocity and torque of the motor. Such a link in the first order equation (5) can influence the phase angle between the input and output in the range ψ=0-π/2. Note that a small value of the dissipation phase angle ψ does not significantly affect the frequency of the oscillations. Nevertheless, in calculating the power dissipation, the phase angle must be taken into account. As a result, equation (8) can be represented by

$$E_{e-mech\_i} = \frac{1}{T_i}\int_0^{T_i} [T_{motor} \cdot \phi_{1i} \sin(\omega_i t) \cdot \sin(\omega_i t + \psi_i)\, dt = 0.5 \cdot [p\,|W(\omega_i)|^2\, \phi_{1i}^2] =$$
$$= 0.5\, p_{equili\_i} \cdot \phi_{1i}^2, \quad p_{equili\_i} = p\,|W(\omega_i)|^2 = p/(\tau_e \omega_i)^2 + 1 \quad (9)$$

where p_{equili_i} is the dynamic slope coefficient of the traction characteristics of motor that depends on the electrical machine's time constant τ_e and frequency of the vibration of the rotor ω_i.

The total average power E_d dissipated in the motor during the oscillations can be computed using:

$$E_d = E_{mech} + E_{e-mech\_i} = 1/2\,[c_{e-m} \cdot \phi_1^2(t) + c_1 \cdot (\phi_1(t) - \phi_2(t))^2 + c_2 \cdot (\phi_2(t) - \phi_1(t))^2 +$$
$$+ (p/(\tau_e \omega_i)^2 + 1) \cdot \phi_{1i}^2]. \quad (10)$$

The condition at which the input energy generated by self-excited vibration and the dissipated energy are equal $E_{self} = E_d$, and the system is on the stability boundary (Fig. 4a) takes the following form:

$$\eta(\dot{\varphi}_2^2(t)-\dot{\varphi}_3^2(t))=c_{e-m}\cdot\dot{\varphi}_1^2(t)+c_1\cdot(\dot{\varphi}_1(t)-\dot{\varphi}_2(t))^2+c_2\cdot(\dot{\varphi}_2(t)-\dot{\varphi}_1(t))^2+ p/(\tau_e\omega_i)^2+1\cdot\dot{\varphi}_{1i}^2. \tag{11}$$

Using the values of the coefficients of forms of vibration that correspond to the boundary damping $\bar{c}_i$ for the oscillations with the natural frequency ω_i, the equation (11) can be written by:

$$\bar{c}_i=\frac{\eta(\mu_{2i}^2(t)-\mu_{3i}^2(t))-c_2\cdot(\mu_{2i}^2(t)-\mu_{3i}^2(t))-c_{e-m}\cdot\mu_{1i}^2(t)-(p/(\tau_e\omega_i)^2+1)\cdot\mu_{1i}^2}{(\mu_{1i}(t)-\mu_{2i}(t))^2+(\mu_{2i}(t)-\mu_{1i}(t))^2} \tag{12}$$

The natural frequencies of oscillations in the considered drive can be computed by using the equation

$$(k_1-I_M^2\cdot\omega^2+k_{em})\cdot(k_2^2-(k_1+k_2+I_{kl}\cdot\omega^2)(k_2+I_{kp}\cdot\omega^2)=0. \tag{13}$$

where the coefficients of the natural forms are as follows:

$$\mu_{1i}=1,\ \mu_{2i}=\frac{k_1+k_{e-m}}{-\omega_i^2 I_M+k_1},\ \mu_{3i}=\frac{k_2}{-\omega_i^2 I_{kp}+k_2}. \tag{14}$$

In the case of the considered traction drive model, the coefficients of natural forms (14) depend on the inertial parameters of drive I_M, I_{kp} and stiffness coefficients k_1, k_2, $k_{e\text{-}m}$.

For the assumption that the damping in the wheelset is a small number and can be neglected (c_2=0), the equation (12) can be written as follows:

$$\bar{c}_i=\frac{\eta(\mu_{2i}^2(t)-\mu_{3i}^2(t))-c_{e-m}\cdot\mu_{1i}^2(t)-(p/(\tau_e\omega_i)^2+1)\cdot\mu_{1i}^2}{(\mu_{1i}(t)-\mu_{2i}(t))^2+(\mu_{2i}(t)-\mu_{1i}(t))^2}. \tag{15}$$

The expression (15) for the low-frequency mode of vibration becomes:

$$\bar{c}_1=\frac{\eta(1-\mu_{3i}^2(t))-c_{e-m}\cdot\mu_{1i}^2(t)-(p/(\tau_e\omega_i)^2+1)}{2(\mu_{2i}(t)-1)^2}. \tag{16}$$

Furthermore, the expression (15) for the high-frequency mode of vibration can be written as:

$$\bar{c}_2=\frac{2\eta(1+\mu_{3i}^2(t))-c_{e-m}\cdot\mu_{1i}^2(t)+(p/(\tau_e\omega_i)^2+1)}{(\mu_{2i}(t)-1)^2}. \tag{17}$$

In the numerical study, we considered a railway drivetrain system with torsionally flexible hollow shaft. The wheelset of the total weight of 1700 kg and the loads for the wheels of Q_1=Q_2=42 kN are assumed. The wheelset is driven by the DC motor by means of the hollow shaft with the torsional stiffness and damping coefficient k_1=3000 kNm and c_1=100 Ns/m, respectively. It is assumed that the radius of the wheelset axle and the length of the axle is respectively equal to 0.07 m and 1.6 m. The torsional stiffness of this axis was determined as k_2=14e7 Nm/rad. The remaining parameters used in the simulations are summarised in Table 1.

Tab. 1

Simulation base parameters

η, kNms	$c_{e\text{-}m}$, Ns/m	c_2, Ns/m	p, kNms	I_M, kgm^2	$I_{kl} = I_{kr}$, kgm^2	τ_e, s
10	4	50	20	2.1	78	0.01

Applying equations 13 and 14 for the considered railway drive, we can demonstrate the natural frequencies of the system as functions of the stiffness of the wheelset k_2 and stiffness of the connection between the electric drive and wheelset k_1 (Fig. 5). The influence of skipping of the stiffness coefficient k_{em} associated with the electromagnetic field of electric motor on the dynamics of the considered drive system is marked on the charts (Fig. 5) by k_{em}=0.

Using equations 15-17 obtained from the analysis of the railway drivetrain's model are plotted the regions of existence of torsional self-vibration by the consideration and non-consideration of the damping coefficient associated with the electromagnetic field of electric motor ($c_{em} \neq 0$ and c_{em}=0) (Fig. 6). The chart demonstrates four areas I, II, III, IV corresponding to different types of vibrations.

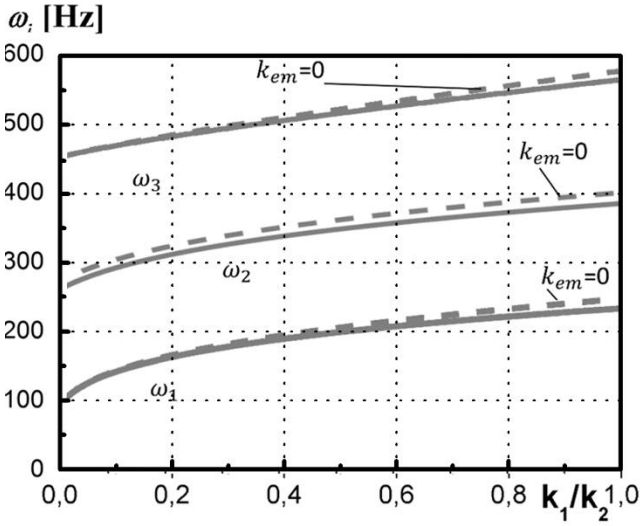

Fig. 5. The natural frequencies of existence of torsion vibration in the traction drive as a function of the relationship k_1/k_2

Comparing the obtained results with those presented in the paper [12], a qualitative match can be observed. Analysing the waveforms presented in Figure 5, it can be concluded that if the damping coefficient c_2 in the driveline takes value located below the line $\bar{c}_1$, then the system is sensitive to low frequency torsional vibrations. On the other hand, if the value of c_2 is within the region located below the line $\bar{c}_2$, then the high self-excited torsional vibrations can be observed.

Summarising the results, it can be concluded that in the region I, only the high-frequency self-excited vibration may occur. The value of damping c_2 in the region II can induce the low-frequency self-excited torsional vibrations. In region III, the self-excited torsional vibrations cannot occur. Finally, in region IV, both types of vibrations mentioned above may be induced.

It is worth mentioning that if we omit the damping c_{em} generated by the electromagnetic field in the model of DC motor, then the region IV expands its area. In the same time, the area of the region I shrinks.

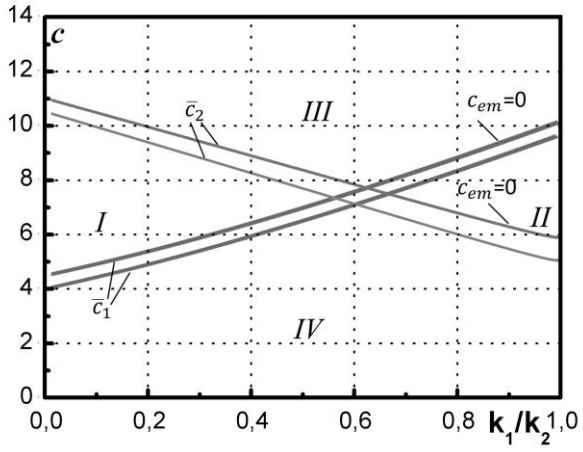

Fig. 6. The regions of low-, high- and self- excited torsional vibrations in the considered driveline

4. SUMMARY AND CONCLUSION

The obtained results demonstrated that the electromagnetic transient processes generated in the electric motor should be taken into account when analysing the stability of the system. The knowledge about the stability of drive transmission systems of railway vehicles is of great importance in the field of dynamics and material fatigue of the drive systems component.

In this paper, a dynamic interaction between the torsionally vibrating railway wheelset and rotor of driving DC motor was investigated. Based on the method of the energy balance of the natural modes as described in detail in this paper [12], the analysis on the oscillations of a railway driveline takes into account the influence of electromagnetic parameters on its stability in relation to self-excited torsional vibration generated by adhesion in the wheel-rail zone.

From the viewpoint of the transient and steady state dynamic responses, particular attention was focused on the influence of the dynamic properties of the mechanical system as well as selected electromagnetic parameters of the electric motor. In the analysed case, special attention was focused on the stiffness and damping coefficients associated with the electromagnetic field of the DC motor. The less the mechanical damping in the driven system, the greater the possibility of severe torsional resonances, particularly when in such a drive train, a semi-elastic connection as hollow shaft with a linear characteristic is used. The obtained results can serve for the design of the driven systems and be helpful for their users during regular maintenance.

Reference

1. Amezquita-Brooks Luis, Eduardo Liceaga-Castro, Jesus Liceaga-Castro. 2014. “Novel design model for the stator currents subsystem of induction motors”. *Applied Mathematical Modelling* 38(23): 5623-5634. ISSN 0307-904X.

2. Bogacz Roman, Kurt Frischmuth. 2016. “On dynamic effects of wheel–rail interaction in the case of Polygonalisation”. *Mechanical Systems and Signal Processing* 79: 166-173. ISSN: 0888-3270. DOI: 10.1016/j.ymssp.2016.03.001.
3. Czech Piotr. 2012. „Determination of the course of pressure in an internal combustion engine cylinder with the use of vibration effects and radial basis function - preliminary research”. *Communications in Computer and Information Science* 329: 175-182. DOI: https://doi.org/10.1007/978-3-642-34050-5_21. Springer, Berlin, Heidelberg. ISBN: 978-3-642-34049-9. ISSN: 1865-0929. In: Mikulski Jerzy (eds), *Telematics in the Transport Environment, 12th International Conference on Transport Systems Telematics*, Katowice Ustron, Poland, October 10-13, 2012.
4. Czech Piotr. 2011. „Diagnosing of disturbances in the ignition system by vibroacoustic signals and radial basis function - preliminary research”. *Communications in Computer and Information Science* 239: 110-117. DOI: https://doi.org/10.1007/978-3-642-24660-9_13. Springer, Berlin, Heidelberg. ISBN: 978-3-642-24659-3. ISSN: 1865-0929. In: Mikulski Jerzy (eds), *Modern Transport Telematics, 11th International Conference on Transport Systems Telematics*, Katowice Ustron, Poland, October 19-22, 2011.
5. Duda Sławomir. 2014. “Numerical simulations of the wheel-rail traction forces using the electromechanical model of an electric locomotive”. Journal *Theoretical and* Applied Mechanics 52(2): 395-404.
6. Eugene I. Rivin. 1999. *Stiffness and damping in mechanical design*, CRC Press, pages 528. DOI:10.1115/1.802939.
7. Haniszewski Tomasz. 2017. “Modeling the dynamics of cargo lifting process by overhead crane for dynamic overload factor estimation”. *Journal of Vibroengineering* 19(1): 75-86. DOI: 10.21595/jve.2016.17310. ISSN: 1392-8716.
8. Haniszewski Tomasz, Damian Gaska. 2017. “Numerical modelling of I-Beam jib crane with local stresses in wheel supporting flanges - influence of hoisting speed”. *Nase More* 64(1): 7-13. DOI: 10.17818/NM/2017/1.2. ISSN: 0469-6255.
9. Henao Humberto, Shahin Hedayati Kia, Gérard-André Capolino. 2011. “Torsional-vibration assessment and gear-fault diagnosis in railway traction system”. *IEEE Trans. Ind. Electron*. 58(5): 1707-1717. ISSN: 0278-0046. DOI: 10.1109/TIE.2011.2106094.
10. Jára Miloslav. 2017. “Introduction to the Influence of Torsional Oscillation of Driving Wheelsets to Wheel/Axle Press-fitted Joint”. *Conference proceedings of Student's Conference STC.* P. 17-26.
11. Jouch Lieh, Jan Yin. 1998. “Stability of a Flexible Wheelset for High Speed Rail Vehicles With Constant and Varying Parameters”. *Journal of Vibration and Acoustics* 120(4): 997-1002. ASME. DOI: 10.1115/1.2893933.
12. Klorkopet Peter. z. 2014. “The Incfinlualencle of Electromagnetic Processes on Stapbility of Loiclomotives Traction Drive in The Slipping Mode”. *Transalport Problems* 9 (2): 41-48.
13. Mei T.X., I. Hussain. 2010. “Detection of wheel-rail conditions for improved traction control”. *Railway Traction Systems (RTS 2010) IET Conference* 1(6): 13-15. DOI:10.1109/Control.2012.6334713.
14. Pochanke Andrzej. 2008. „Engines induced with permanent magnet in applying to the drive of traction vehicles”. *TTS - Rail Transport Technique* 14(5-6): 22-25.
15. Shahin Hedayati Kia, Humberto Henao, Gérard-André Capolino. 2009. “Torsional vibration assessment in railway traction system mechanical transmission”. 2009 IEEE International Symposium on Diagnostics for Electric Machines, Power Electronics and Drives. P. 1-8. ISBN: 978-1-4244-3441-1. DOI: 10.1109/DEMPED.2009.5292750.

16. Vectron – the drive system. Siemens.com Global Website.
17. Voltr Petr, Michael Lata, Ondřej Černý. 2012. "Measuring of wheel-rail adhesion characteristics at a test stand". In: *Proceedings of XVIII International Conference on Engineering Mechanics*. Czech Republic.
18. Winterling M.W., E. Tuinman, W. Deleroi. 1998. "Simulation of drive line dynamics of light-rail vehicles". In: *Simulation '98. International Conference.* Conf. Publ. No. 457. IET. P. 79-84. DOI:10.1049/cp:19980619.
19. Xu Kun, Zeng Jing, Wei Lai. 2019. "An analysis of the self-excited torsional vibration of high-speed train drive system". *Journal of Mechanical Science and Technology* 33(3): 1149-1158.

Received 15.09.2019; accepted in revised form 05.11.2019